Spectral and temporal metrology with band-limited functions and finite-time measurements

Łukasz Rudnicki[*] and Tomasz Linowski

International Centre for Theory of Quantum Technologies, University of Gdańsk, Jana Bażyńskiego 1A, 80-309 Gdańsk, Poland

We perform an analysis supplementing the metrology toolbox in the time-frequency domain. While the relevant time-frequency-based metrological protocols can be borrowed from the spatial domain, where they have recently been well developed, their ultimate practical usefulness is shown to be restricted by limits put on the bandwidth of both the signal and measurements, as well as by the finite measurement time. As we demonstrate for the well-known problem of multiparameter estimation for two incoherent, pointlike sources, the impact of these experimental limitations on the optimal protocol's efficiency can be detrimental. Nonetheless, we propose necessary operational criteria for attainability of the quantum Cramér-Rao bound under the discussed restrictions.

I. INTRODUCTION

Time and frequency form a pair of variables which is *conjugate* in the sense that, already in classical signal analysis, they are connected by Fourier transform. In the quantum framework, their mutual relation is thus very similar to the one between spatial variables: position and momentum, also connected by the Fourier transform. However, while developing a time-frequency counterpart of a notion established for the position-momentum pair, such as a toolbox for quantum metrology, careful thought due to subtle differences between the space-momentum regime and the time-frequency domain is required.

Even though it is widely known that an operator corresponding to time does not exist (this is because frequencies are non-negative, in the same vein as energy), such a restriction does not prevent a comprehensive phase-space description of time and frequency in terms of the Wigner function [1]. Construction of a complete set of gates also does not pose issues, since the gates can literally be adapted from the ones in the position-momentum phase space [1].

As a consequence, the existing metrology toolbox developed for position and momentum can be also applied to problems relying on time and frequency measurements. A prime example of such a metrological scenario, which can be solved due to quantum-inspired techniques, concerns two closely separated, incoherent pointlike light sources [2–4], relevant for, e.g., resolving starlight and exoplanet detection [5,6]. In such a case, the usual goal is to estimate the sources' relative separation [7–12] or, in the most general, multiparameter case, their separation simultaneously with relative brightness and the centroid [13,14]. As has been theoretically proven and experimentally verified, the very same problem phrased in the time domain admits an analogous solution [15,16]. Similar conclusions apply to other scenarios, such as

continuous variable tomography [17,18]: the same techniques that are used to restrict tomography protocols to a finite spatial subspace spanned by a fixed set of Hermite-Gauss (HG) or Laguerre-Gauss modes can be applied to the time or frequency domain, where the HG modes are a basic tool [19]. In short, from a practical point of view, the transfer of spatial metrology techniques to the time-frequency domain is mostly straightforward.

Nonetheless, the different character of the time-frequency pair (in comparison with the position-momentum pair) does impose certain limiting factors. Taking into account the experimental conditions, in this work, we identify and analyze two salient features of metrology in the time-frequency domain:

(i) finite bandwidth Ω,

(ii) finite measurement time $2T$.

As we show, depending on the value of a single parameter ΩT, the above restrictions can have significant impact on the efficiency of time-frequency protocols borrowed from the spatial domain, including the previously discussed multiparameter estimation for two incoherent sources. To derive our findings, we develop a set of tools for time-frequency metrology based on so-called *spheroidal wave functions* known from signal analysis [20–22].

This paper is organized as follows. In Sec. II, we review the basic properties of the spheroidal wave functions. In Sec. III, we discuss the general metrology-oriented consequences of time- and band-limiting. These results are then applied by us in Sec. IV to derive limits on temporal superresolution obtained from well-proven protocols known from the spatial domain. Finally, in Sec. V, we provide an outlook.

II. PROLATE SPHEROIDAL WAVE FUNCTIONS

Spheroidal wave functions of various kinds are related to the solutions of the Helmholtz equation in prolate or oblate spheroidal coordinates. Due to their unique properties, they are also ubiquitous in signal analysis, where they were introduced by Slepian and Pollack [20]. There are many sources,

---

[*]Contact author: lukasz.rudnicki@ug.edu.pl

summarizing various useful properties of these functions. In this very brief introduction we rely on the pedagogical presentation from Ref. [21], though we will slightly change the notation to fit our problem.

Let Ω be a bandwidth and $2T$ be the length of time interval $[-T, T]$. Prolate spheroidal wave functions (PSWFs) $\psi_n(c, t)$ are solutions of the following integral equation:

$$\int_{-T}^{T} dz \frac{\sin[\Omega(t-z)]}{\pi(t-z)} \psi_n(c, z) = \lambda_n(c) \psi_n(c, t), \quad (1)$$

where $n = 0, 1, 2, \ldots$ and we stress that the domain of the PSWFs is the whole real number line, not just the interval $[-T, T]$. The dimensionless parameter $c = \Omega T$ (not to be confused with the speed of light), also sometimes called the *Slepian frequency*, provides a single number characterizing the system. If $c \gg 1$, potential effects due to time- and band-limiting are negligible. Moreover, it is enough to relax just one of these constraints to reach the limit $c \to \infty$.

The eigenvalues $0 \leqslant \lambda_n \leqslant 1$, given by the formula

$$\lambda_n(c) = \frac{2c}{\pi} [R_{n0}(c, 1)]^2, \quad (2)$$

are ordered decreasingly. In the limit $c \to \infty$, they all approach the unity; however, the largest eigenvalue λ_0 equals approximately 0.999 already for $c = 5$.

The quantities $R_{n0}(c, z)$ are radial spheroidal functions of the first kind. While there are many platforms suitable for numerical studies of these functions, for the sake of clarity and consistency it is useful to mention that, in MATHEMATICA [23], we have the correspondence

$$R_{n0}(c, z) \equiv \text{SpheroidalS1}[n, 0, c, z].$$

The wave functions $\psi_n(c, z)$ are appropriately normalized versions of $S_{n0}(c, z/T)$, with the latter being angular spheroidal functions of the first kind. For completeness, let us mention that in MATHEMATICA they are denoted by

$$S_{n0}(c, z) \equiv \text{SpheroidalPS}[n, 0, c, z],$$

provided that the normalization of the angular functions is chosen to be

$$\int_{-1}^{1} dz [S_{n0}(c, z)]^2 = \frac{2}{2n+1}.$$

Here, we adopt the following normalization of the solutions of Eq. (1):

$$\psi_n(c, z) = \sqrt{\frac{\lambda_n(c)}{T \int_{-1}^{1} dz' [S_{n0}(c, z')]^2}} S_{n0}\left(c, \frac{z}{T}\right),$$

so that the relations of "double orthogonality" hold:

$$\int_{-\infty}^{\infty} dz \psi_n(c, z) \psi_m(c, z) = \delta_{nm}, \quad (3)$$

$$\int_{-T}^{T} dz \psi_n(c, z) \psi_m(c, z) = \lambda_n(c) \delta_{nm}. \quad (4)$$

From the latter relation we can see that the eigenvalues $\lambda_n(c)$ quantify the amount of the corresponding PSWF contained within the interval $[-T, T]$.

An important property of PSWFs concerns their usage as an orthonormal basis for band-limited functions. The function

$f(t)$ can be expanded as

$$f(t) = \sum_{n=0}^{\infty} f_n \psi_n(c, t) \quad (5)$$

with some coefficients f_n if and only if its Fourier transform $\tilde{f}(\omega)$ is supported on $[-\Omega, \Omega]$. This means that Eq. (5) is a natural way to impose the constraint of limited bandwidth on a function, which we make frequent use of below. We remark that the expansion is valid for every finite T, though the coefficients f_n do depend on the choice of the time limit.

To gain some intuition behind the above decomposition, let us point out the asymptotic connection between the PSWF and the Hermite-Gauss (HG) modes; the latter are explicitly defined as

$$\psi_n^{\text{HG}}(c, z) = \left(\frac{c}{\pi}\right)^{1/4} \frac{e^{-cz^2/2}}{\sqrt{2^n n!}} H_n(\sqrt{c}z), \quad (6)$$

where the variance of the modes equals $\sigma^2 = 1/(2c)$ and $H_n(x)$ is the nth Hermite polynomial. Then, for $c \gg 1$, it is known that [24]

$$\psi_n(c, z) \approx \psi_n^{\text{HG}}(c, z). \quad (7)$$

See Fig. 1 for an illustration of this effect. This result is a special case of a more general branch-dependent asymptotic expansion of the PSWFs. As we can see, if c is sufficiently large, Eq. (5) is simply a standard decomposition of the function $f(t)$ in the basis formed by narrow HG modes.

III. METROLOGY WITH TIME AND BAND LIMITATIONS

A generic protocol of quantum metrology consists of a probe state $\hat{\varrho}_{\theta}$, in which parameters of interest [denoted by $\theta = (\theta_1, \theta_2, \ldots)$] are being encoded, and a positive operator valued measure (POVM), which describes the measurement used to reveal the values of the parameters [25]. The latter, for the sake of manageability, can be considered as consisting of a finite number d of operators $\hat{\Pi}_i$, for $i = 0, \ldots, d-1$. Due to information completeness, the last operator reads $\hat{\Pi}_d = \mathbb{1} - \sum_{i=0}^{d-1} \hat{\Pi}_i$.

Both the probe state $\hat{\varrho}_{\theta}$ and the POVM elements $\hat{\Pi}_i$ can be decomposed in various ways in accord with the Schrödinger mixture theorem, in particular, in terms of their eigendecompositions. Let us, therefore, write

$$\hat{\varrho}_{\theta} = \sum_k \varrho_k |\Psi_k\rangle\langle\Psi_k|, \quad (8)$$

$$\hat{\Pi}_i = \sum_l \Pi_{il} |\pi_{il}\rangle\langle\pi_{il}|. \quad (9)$$

Information about the parameters θ can be then accessed through probabilities

$$p_i = \text{Tr}(\hat{\varrho}_{\theta} \hat{\Pi}_i) = \sum_{k,l} \varrho_k \Pi_{il} |\langle\pi_{il}|\Psi_k\rangle|^2, \quad (10)$$

for $i = 0, \ldots, d-1$. Obviously $p_d = 1 - \sum_{i=0}^{d-1} p_i$. We remark that in optical considerations (like in the next section), the probe states $\hat{\varrho}_{\theta}$ are typically restricted to mixtures of single-photon states, with $|\Psi_k\rangle$ referring to single-photon states of the associated temporal modes.
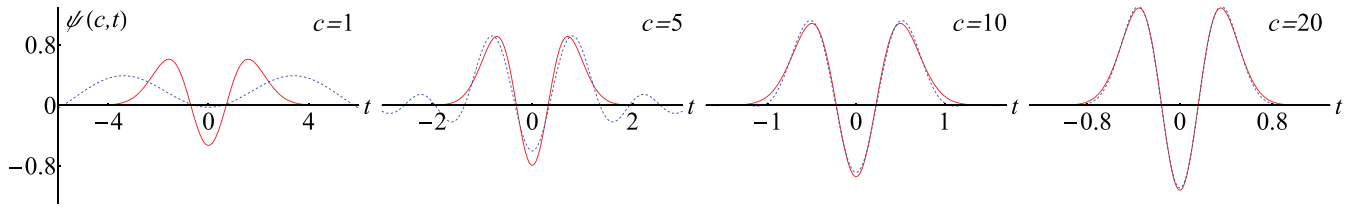
FIG. 1. Comparison between the second prolate spheroidal wave function $\psi_2(c,t)$ (blue, dashed line) and the second Hermite-Gauss mode $\psi_2^{\mathrm{HG}}(c,t)$ (red line) for $c \in \{1, 5, 10, 20\}$, starting from the left and increasing to the right. The vertical axis is shared by all four plots. As we can see, for $c = 1$ there is a severe discrepancy between the functions, while for $c = 10$ the difference is almost unnoticeable.

The efficiency of the protocol is quantified by the generalization of the Cramér-Rao bound [26–28] to multiparameter estimation [29,30]. For a given measurement scheme, each of the parameters can be, in principle, measured with uncertainty not smaller than

$$\Delta \theta_n \geqslant \sqrt{(F^{-1})_{nn}(\boldsymbol{\theta})}, \tag{11}$$

where F is the (classical) Fisher information matrix [31]:

$$F_{nm} = \sum_j \frac{1}{p_j} \frac{\partial p_j}{\partial \theta_n} \frac{\partial p_j}{\partial \theta_m}. \tag{12}$$

In the case of a single parameter, one can optimize over all POVMs to obtain the quantum Fisher information matrix, which saturates the Cramér-Rao bound, corresponding to the ultimate resolution allowed by quantum mechanics [29,30]. In the case of more than one parameter, optimal measurements for different parameters may be mutually incompatible, preventing the Cramér-Rao bound from being saturated [32]. Finding the general necessary and sufficient conditions under which the multiparameter quantum Fisher information matrix is attainable remains an open problem in quantum information theory [33].

To incorporate both practical limitations under consideration, let us first note that in continuous variable systems, all pure states $|\phi\rangle$ can be further described in terms of wave functions. For example, in the position domain, the wave function is given by $\phi(x) = \langle x|\phi\rangle$. The same construction does hold in the time or frequency domain [19]. Without loss of generality, let us focus on the time domain.

Following the above notation, the probe state is described by a collection of wave functions $\Psi_k(t)$, while the POVM elements are given by $\pi_{il}(t)$. Their properties are the same as for the position domain, with one important caveat: limited bandwidth implies that all functions $\Psi_k(t)$ and $\pi_{il}(t)$ are band-limited too; i.e., their Fourier transforms "living" in the frequency domain must be finitely supported. This assertion holds independently of the assumed convex decompositions of the probe state and the POVMs.

The restriction to band-limited functions can be explicitly imposed on the wave functions associated with the probe and with the POVMs by decomposing them according to Eq. (5):

$$\Psi_k(t) = \sum_{n=0}^{\infty} \Psi_{kn} \psi_n(c,t), \tag{13}$$

$$\pi_{il}(t) = \sum_{n=0}^{\infty} \pi_{iln} \psi_n(c,t). \tag{14}$$

Then, due to the orthogonality of the PSWFs on the whole real line (3), the probabilities (10) take the form

$$p_i = \sum_{k,l} \varrho_k \Pi_{il} \left| \sum_{n=0}^{\infty} \pi_{iln}^* \Psi_{kn} \right|^2. \tag{15}$$

Note that for large c this expansion is the same as if we used narrow HG modes.

In addition to finite bandwidth, we need to account for the fact that the measurement occurs in a finite-time interval, here denoted as $[-T, T]$. To this end, we introduce a projector onto this interval, denoted by $\hat{\Xi}_T$. For an arbitrary pure state $|\phi\rangle$ with its wave function $\phi(t)$, the action of this operator gives the state $\hat{\Xi}_T|\phi\rangle$, whose wave function equals $\phi(t)$ for $t \in [-T, T]$ and vanishes outside of this interval (of course, for $T \to \infty$, the wave function is untouched). Such a wave function is no longer normalized, and its norm is in general smaller than 1. When calculating expectation values, we can think of $\hat{\Xi}_T$ as being represented by

$$\hat{\Xi}_T = \int_{-T}^{T} dt\, |t\rangle\langle t|, \tag{16}$$

with $|t\rangle$ being orthonormal vectors such that, for any $|\phi\rangle$, we have $\langle t|\phi\rangle = \phi(t)$.

While the normalization of the probe state must be intact, the same does not need to hold for the POVM elements. At the end, the "leakage" element $\hat{\Pi}_d$ subsumes all information which has not been captured by the measurements. In other words, while we are not allowed to model the finite time of the measurement by truncating the probe state, we can replace the POVM elements (except the last one) according to the rule

$$\hat{\Pi}_i \mapsto \hat{\Xi}_T \hat{\Pi}_i \hat{\Xi}_T. \tag{17}$$

To incorporate this replacement inside the measurement probabilities we resort to the second orthogonality condition (4). As a result, taking into account both limitations, the probabilities (15) become

$$p_i = \sum_{k,l} \varrho_k \Pi_{il} \left| \sum_{n=0}^{\infty} \pi_{iln}^* \Psi_{kn} \lambda_n(c) \right|^2, \tag{18}$$

where we stress that the equation applies only to $i = 0, \ldots, d-1$. Note also the presence of $\lambda_n(c)$ inside the absolute value.

Physical intuition behind the steps taken above is the following. First, through Eqs. (13) and (14), we impose the restriction of being band-limited to both the probe state and
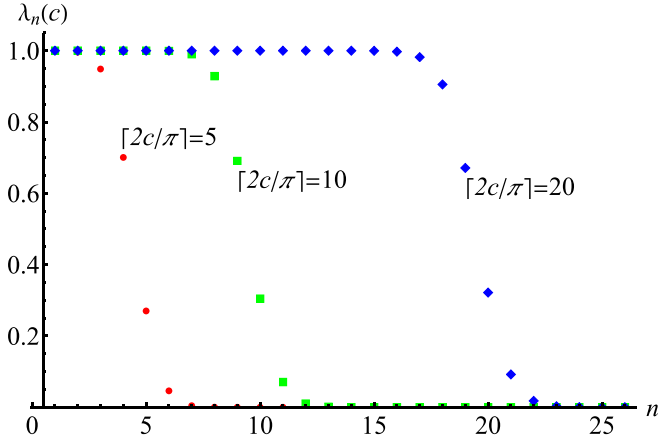
FIG. 2. Eigenvalues $\lambda_n(c)$ shown as a function of n (on the horizontal axis), for c such that $\lceil (2c)/\pi \rceil = \{5, 10, 20\}$ (red circles, green squares, and blue diamonds, respectively). As can be seen, the eigenvalue is almost equal to unity starting from $n = 0$ and up to approximately $n = \lceil (2c)/\pi \rceil$, around which we observe a sudden decay involving three to four eigenvalues. The rest of the spectrum is approximately vanishing.

the measurements. Without this assumption, we are, in principle, allowed to generate arbitrarily narrowly localized signals (probe states) and perform arbitrarily narrow measurements. The second step, captured by Eq. (17), accounts for the fact that the measurement does not last "forever." So even though the signal can extend beyond (especially before) the measurement starts, the measurement itself happens in a finite-time window.

As previously discussed, the extent to which the two restrictions affect the measurement is ultimately captured by a single parameter, the Slepian frequency c. In Ref. [16], for example, the bandwidth and measurement time characterizing the experiment equaled 17 GHz and 20 μs, resulting in $c \approx 10^5$, way above the negligibility threshold $c \gg 1$. However, in that same paper, the true accessible timescale was reported to be of the order of 30 fs, which would correspond to the radically small $c \approx 10^{-4}$, given the same bandwidth. With a growing need for enhanced measurement efficiency and precision, we predict the latter regime to be gradually approached, necessitating taking the discussed restrictions into account.

To infer meaningful conclusions of general validity we resort to a very handy property of the eigenvalues $\lambda_n(c)$. As is well known [21], with the exception of relatively small values of c, the first $\lceil (2c)/\pi \rceil$ eigenvalues are very close to 1, while the remaining eigenvalues quickly drop to 0. This behavior can be observed in Fig. 2. Given this, our previous result (18) can be faithfully approximated as

$$p_i \approx \sum_{k,l} \varrho_k \Pi_{il} \left| \sum_{n=0}^{\lceil (2c)/\pi \rceil} \pi_{iln}^* \Psi_{kn} \right|^2. \quad (19)$$

An underpinning of this equation can serve as a litmus paper for optimality in a quantum metrology protocol, the latter being understood as saturation of the quantum Cramer-Rao bound (11).

To this end, given a probe state, one shall look for a POVM saturating this bound. Assuming that such a POVM has been found, we need to expand it in the PSWF basis. As long as it is enough to consider only first $\lceil (2c)/\pi \rceil$ terms of this expansion, optimality is preserved. In other words, we shall require that the optimal POVM fulfills

$$\pi_{il}(t) \approx \sum_{n=0}^{\lceil (2c)/\pi \rceil} \pi_{iln} \psi_n(c, t). \quad (20)$$

This is true because probabilities relevant for the discussed measurement circumstances, which turn out to be well approximated by Eq. (19), do not differ from the probabilities obtained in an infinitely long experiment. However, when higher-order terms are necessary to describe the optimal POVM elements faithfully, we know that optimality is lost. What might be even more striking is that there is no other choice for a POVM, which would be able to restore optimality. Had that been possible, we would have already started with an optimal POVM sufficiently well approximated by the terms of the order not higher than $\lceil (2c)/\pi \rceil$.

IV. LIMITS ON TEMPORAL SUPERRESOLUTION

To demonstrate the potential effect of time- and band-limiting in practical scenarios, we consider the problem of resolving temporal separations between two pointlike incoherent light pulses.

As discussed previously in the Introduction, in the absence of time and band limitations, the scenario is fully analogous to the well-known problem of resolving spatial separations between light sources [7–14] and hence can be modeled in a similar fashion [15,16]. Assuming that the pulses have relative intensities ν and $1 - \nu$ (so that the total intensity is normalized to 1) and that they are temporally separated by τ with centroid τ_0, the total signal is represented by the following density operator [14]:

$$\hat{\varrho}_{\boldsymbol{\theta}} = \nu |\Psi_+\rangle\langle\Psi_+| + (1 - \nu)|\Psi_-\rangle\langle\Psi_-|, \quad (21)$$

with the parameters of interest being $\boldsymbol{\theta} = (\tau, \tau_0, \nu)$. Here, $|\Psi_\pm\rangle$ are τ-displaced states of the amplitude point spread function $\Psi(t)$ describing the pulses, defined in such a way that $\langle t|\Psi_\pm\rangle = \Psi_\pm(t) = \Psi(t - \tau_0 \mp \tau/2)$, with τ_0 being the signal's centroid. See Fig. 3 for illustration. Note that $\Psi(t)$ is assumed to be real-valued. We remark that, although usually only the separation is of practical significance, in practice it cannot be reliably measured without simultaneously treating the remaining two parameters, hence the need for multiparameter estimation.

For the problem at hand, it was found in Ref. [14] that the quantum Fisher information, saturating the Cramér-Rao bound (11), is achieved with the following scheme. To start with, one needs to define a basis in the signal space. A convenient choice arises by considering the set $\{|\Gamma_n\rangle\}$, defined by

$$\langle t|\Gamma_n\rangle = \frac{\partial^n}{\partial t^n}\Psi(t - \tau_0). \quad (22)$$

From this, an orthonormal basis $\{|\Phi_n\rangle\}$ is obtained by means of the standard Gram-Schmidt process. Then, the optimal POVM set consists of four elements: the first three ($j = 0$,
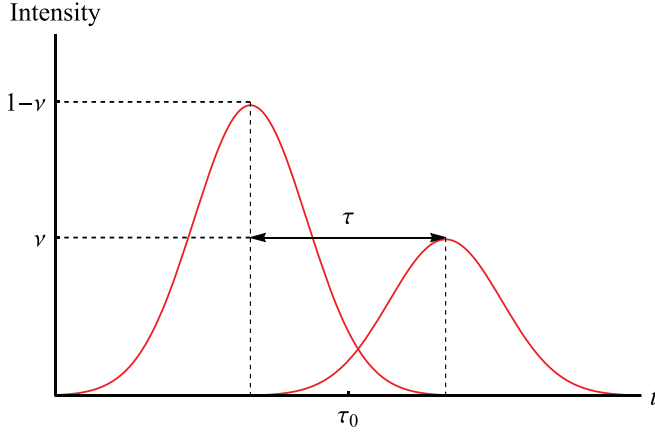
Intensity

FIG. 3. Illustration of the problem of resolving temporal separations between two pointlike incoherent light pulses. Two incoherent signals characterized by different intensities v and $1 - v$ are centered at τ_0 and temporally separated by τ (the latter assumed to be very small). The goal is to simultaneously estimate all three parameters with the best possible precision. In the optimal scheme, the measurement consists of projections onto a set constructed from the Hermite-Gaussian modes, like the one in Fig. 1.

1, and 2) being projectors $\hat{\Pi}_j = |\pi_j\rangle\langle\pi_j|$ of the form

$$|\pi_j\rangle \equiv \sum_{k=0}^{3} C_{jk}|\Phi_k\rangle, \tag{23}$$

and the last defined as $\hat{\Pi}_3 = \hat{\mathbb{1}} - \hat{\Pi}_0 - \hat{\Pi}_1 - \hat{\Pi}_2$. Here, $C_{jk} = \langle\Phi_k|\pi_j\rangle$ are real coefficients, such that the POVMs are all nonnegative and linearly independent.

As was found in Ref. [14], provided a suitable choice of alignment for the measurement apparatus and as long as[1]

$$C_{00} = C_{10} = 0, \quad C_{01}, C_{11}, C_{02}, C_{12} \neq 0, \tag{24}$$

the Fisher information obtained from this scheme differs from the quantum Fisher information only by a multiplicative factor of

$$\mathscr{A} \equiv \frac{(C_{01}C_{12} - C_{11}C_{02})^2}{C_{01}^2 + C_{11}^2} \leqslant 1. \tag{25}$$

Being dependent on four parameters, one may suspect that the inequality can be easily saturated. Indeed, as reported in Ref. [14], this can be done in infinitely many ways, meaning that there are infinitely many measurements attaining the quantum limit. As we will now show, for measurement that is time- and band-limited, this is no longer possible.

To see this, let us first recall how the above limitations affect the measurement. First, due to band-limiting, all the time-dependent functions have to be decomposable into PSWFs, as in Eq. (5). Notably,

$$\Phi_k(t) = \sum_{n=0}^{\infty} \Phi_{kn}\psi_n(c, t). \tag{26}$$

_____

[1]According to Eq. (13) in Ref. [14], the nonvanishing coefficients should be C_{20} and C_{21}, rather than C_{02} and C_{12}. However, it is clear from their further results that the latter was meant.

Second, due to time-limiting, the POVMs should be replaced according to the rule (17). In particular, this implies the following change in the coefficients defining the POVMs:

$$C_{jk} = \langle\Phi_k|\pi_j\rangle \rightarrow \langle\Phi_k|\hat{\Xi}_T|\pi_j\rangle. \tag{27}$$

This is all we need to prove our claim. Because all the coefficients are real, we have

$$C_{jk}^2 = C_{jk}C_{jk}^* = \langle\Phi_k|\hat{\Xi}_T\hat{\Pi}_j\hat{\Xi}_T|\Phi_k\rangle. \tag{28}$$

In particular,

$$C_{01}^2 + C_{11}^2 = \langle\Phi_1|\hat{\Xi}_T(\hat{\Pi}_0 + \hat{\Pi}_1)\hat{\Xi}_T|\Phi_1\rangle \leqslant \langle\Phi_1|\hat{\Xi}_T|\Phi_1\rangle, \tag{29}$$

where the last step follows from the fact that $\hat{\Pi}_0 + \hat{\Pi}_1 \leqslant \hat{\mathbb{1}}$. The above inequality defines a two-dimensional sphere in the space of (C_{01}, C_{11}) centered at $(0,0)$ and with radius squared $r_1^2 \leqslant \langle\Phi_1|\hat{\Xi}_T|\Phi_1\rangle$. This means that we can parametrize C_{01} and C_{11} as

$$C_{01} = r_1 \sin\phi_1, \quad C_{11} = r_1 \cos\phi_1, \tag{30}$$

where $\phi_1 \neq n\pi/2$, so that neither coefficient vanishes, as required by Eq. (24). In full analogy, for some $r_2^2 \leqslant \langle\Phi_2|\hat{\Xi}_T|\Phi_2\rangle$ and $\phi_2 \neq n\pi/2$,

$$C_{02} = r_2 \sin\phi_2, \quad C_{12} = r_2 \cos\phi_2. \tag{31}$$

Substituting these into Eq. (25) and using elementary properties of trigonometric functions, we obtain

$$\mathscr{A} = r_2^2 \sin^2(\phi_1 - \phi_2) \leqslant r_2^2$$
$$\leqslant \langle\Phi_2|\hat{\Xi}_T|\Phi_2\rangle = \int_{-T}^{T} dt \, \Phi_2^2(t), \tag{32}$$

where in the last step we used Eq. (16). According to the Schwartz's Paley-Wiener theorem [34], any function (other than the constant zero function) whose Fourier transform has finite support cannot be finitely supported itself. This means that, since Φ_2 is band-limited, the right-hand side above is strictly smaller than unity for any finite T, finishing the proof.

A more nontrivial upper bound follows from explicit calculation. Using Eqs. (26) and (4) in the last equation, we get

$$\mathscr{A} \leqslant \sum_{n=0}^{\infty} \Phi_{2n}^2 \lambda_n(c). \tag{33}$$

Since $\lambda_n(c)$ are ordered decreasingly, we can bound the sum from above by replacing all $\lambda_n(c)$ with $\lambda_0(c)$, yielding

$$\mathscr{A} \leqslant \lambda_0(c). \tag{34}$$

Therefore, in the presence of band- and time-limiting, the Fisher information attained from the optimal scheme differs from the ultimate precision allowed by quantum mechanics by a multiplicative factor not larger than the eigenvalue $\lambda_0(c)$. As seen from Fig. 4, despite approaching unity relatively quickly with c, there is still a significant range of values of this parameter, for which the implied limitations are severe.
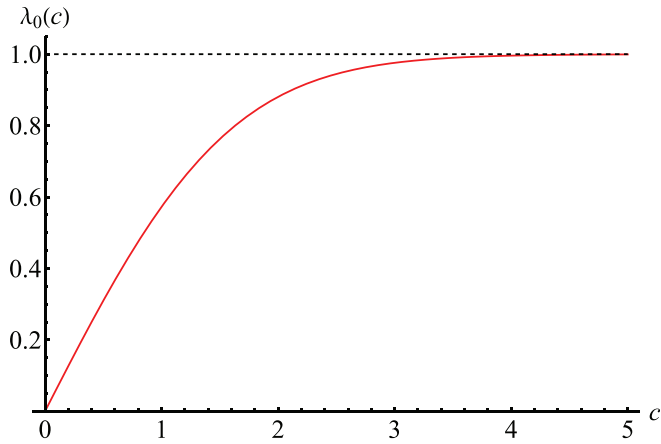
FIG. 4. The largest eigenvalue of PSWFs $\lambda_0(c)$ (red line), constituting an upper bound on the multiplicative factor by which the Fisher information in the optimal measurement scheme differs from the ultimate quantum precision in the presence of band- and time-limiting. For convenience, the ideal value of the multiplicative factor, equal to 1, is denoted by a dashed black line. As seen, for values of c close to 0, the limitations put on superresolution are severe.

Let us furthermore observe that the inequality (34) is saturated only if $\Phi_{2m} = \delta_{m,0}$, i.e., if $\Phi_2(t)$ coincides with the zeroeth PSWF $\psi_0(c, t)$. However, this is highly unlikely as, by construction, $\Phi_2(t)$ is related to the second derivative of the amplitude point spread function, which should be closer to the second or higher PSWF. For example, in the well-known case of a Gaussian point spread function, the ideal $\Phi_2(t)$ corresponds to the second Hermite-Gauss mode, which, due to the asymptotic relation (7), must reduce to a function much closer to the second than the zeroeth PSWF after band-limiting. In short, we expect that in practice, the true implications of time- and band-limiting should be even more severe than demonstrated here. As such, in experiment, special attention should be paid to extend both the bandwidth and the time of each measurement, so as to maximize the efficiency-lowering parameter c.

V. OUTLOOK

Virtually all techniques developed for metrology in the spatial domain can be recontextualized to the time (or frequency) domain in a way which, at least from the theory perspective, is straightforward. However, our analysis, taking into account potential experimental limitations, reveals that during such adaptation the optimality of a given metrology protocol is lost if the dimensionless product of the bandwidth and the time of the measurement c (the Slepian frequency) is too small in comparison with the number of PSWFs with the same Slepian frequency necessary to faithfully reproduce the optimal POVMs. This was demonstrated by us explicitly for multiparameter estimation for two incoherent, pointlike sources, where small values of c had a radical impact on protocol efficiency.

While typical contemporary experiments should be characterized by sufficiently large Slepian frequency, practical problems, such as the need to maximize the number of measurements performed during an allocated time window, or simply lack of appropriate resources, may lead to extreme experimental conditions, in which both the bandwidth and the time of the measurement are pushed to their limits. It is clear that, in such a regime, strategies different to the ones from the spatial domain need to come into play. From a comparison between Eqs. (18) and (19), we can see that a partial solution to the problem is given by a careful preparation of the probe state. If the latter is approximately decomposable into exclusively low order PSWFs, the optimal POVMs will follow this pattern, leading to high protocol efficiency. Specific methods to counteract the detrimental effect of band- and time-limiting shall be considered as the right target for further studies.

[1] N. Fabre, A. Keller, and P. Milman, Time and frequency as quantum continuous variables, Phys. Rev. A **105**, 052429 (2022).

[2] X.-M. Lu, H. Krovi, R. Nair, S. Guha, and J. H. Shapiro, Quantum-optimal detection of one-versus-two incoherent optical sources with arbitrary separation, npj Quantum Inf. **4**, 64 (2018).

[3] Z. Huang and C. Lupo, Quantum hypothesis testing for exoplanet detection, Phys. Rev. Lett. **127**, 130502 (2021).

[4] K. Schlichtholz, T. Linowski, M. Walschaers, N. Treps, Ł. Rudnicki, and G. Sorelli, Practical tests for sub-Rayleigh source discriminations with imperfect demultiplexers, Opt. Quantum **2**, 29 (2024).

[5] J. T. Wright and B. S. Gaudi, Exoplanet detection methods, in *Planets, Stars and Stellar Systems*. Vol. 3: *Solar and Stellar Planetary Systems*, edited by T. D. Oswalt, L. M. French, and P. Kalas (Springer, Dordrecht, 2013), pp. 489–540.

[6] D. A. Fischer, A. W. Howard, G. P. Laughlin, B. Macintosh, S. Mahadevan, J. Sahlmann, J. C. Yee, Exoplanet detection techniques, in *Protostars and Planets VI*, edited by H. Beuther, R. S. Klessen, C. P. Dullemond, and T. Henning (University of Arizona, Tucson, AZ, 2014), p. 715.

[7] M. Tsang, R. Nair, and X.-M. Lu, Quantum theory of superresolution for two incoherent optical point sources, Phys. Rev. X **6**, 031033 (2016).

[8] M. Tsang, Resolving starlight: a quantum perspective, Contemp. Phys. **60**, 279 (2019).

[9] M. Paúr, B. Stoklasa, J. Grover, A. Krzic, L. L. Sánchez-Soto, Z. Hradil, and J. Řeháček, Tempering Rayleigh's curse with PSF shaping, Optica **5**, 1177 (2018).

[10] U. Zanforlin, C. Lupo, P. W. R. Connolly, P. Kok, G. S. Buller, and Z. Huang, Optical quantum super-resolution imaging and hypothesis testing, Nat. Commun. **13**, 5373 (2022).

[11] M. Gessner, C. Fabre, and N. Treps, Superresolution limits from measurement crosstalk, Phys. Rev. Lett. **125**, 100501 (2020).

[12] T. Linowski, K. Schlichtholz, G. Sorelli, M. Gessner, M. Walschaers, N. Treps, and Ł. Rudnicki, Application range of crosstalk-affected spatial demultiplexing for resolving separations between unbalanced sources, New J. Phys. **25**, 103050 (2023).

[13] J. Řeháček, Z. Hradil, B. Stoklasa, M. Paúr, J. Grover, A. Krzic, and L. L. Sánchez-Soto, Multiparameter quantum metrology of incoherent point sources: Towards realistic superresolution, Phys. Rev. A **96**, 062107 (2017).

[14] J. Řeháček, Z. Hradil, D. Koutný, J. Grover, A. Krzic, and L. L. Sánchez-Soto, Optimal measurements for quantum spatial superresolution, Phys. Rev. A **98**, 012103 (2018).

[15] J. M. Donohue, V. Ansari, J. Řeháček, Z. Hradil, B. Stoklasa, M. Paúr, L. L. Sánchez-Soto, and C. Silberhorn, Quantum-limited time-frequency estimation through mode-selective photon measurement, Phys. Rev. Lett. **121**, 090501 (2018).

[16] V. Ansari, B. Brecht, J. Gil-Lopez, J. M. Donohue, J. Řeháček, Z. Hradil, L. L. Sánchez-Soto, and C. Silberhorn, Achieving the ultimate quantum timing resolution, PRX Quantum **2**, 010301 (2021).

[17] J. Řeháček, Z. Hradil, Z. Bouchal, R. Čelechovský, I. Rigas, and L. L. Sánchez-Soto, Full tomography from compatible measurements, Phys. Rev. Lett. **103**, 250402 (2009).

[18] A. I. Lvovsky and M. G. Raymer, Continuous-variable optical quantum-state tomography, Rev. Mod. Phys. **81**, 299 (2009).

[19] B. Brecht, D. V. Reddy, C. Silberhorn, and M. G. Raymer, Photon temporal modes: A complete framework for quantum information science, Phys. Rev. X **5**, 041017 (2015).

[20] D. S. Slepian and H. O. Pollack, Prolate spheroidal wave functions, Fourier analysis and uncertainty—I, Bell Syst. Tech. J. **40**, 43 (1961).

[21] I. C. Moore and M. Cada, Prolate spheroidal wave functions, an introduction to the Slepian series and its properties, Appl. Comput. Harmonic Anal. **16**, 208 (2004).

[22] L.-L. Wang, A review of prolate spheroidal wave functions from the perspective of spectral methods, J. Math. Study **50**, 101 (2017).

[23] Wolfram Research, Inc., MATHEMATICA, Version 13.1, Champaign, IL, 2022.

[24] J. d. Cloizeaux and M. L. Mehta, Some asymptotic expressions for prolate spheroidal functions and for the eigenvalues of differential and integral equations of which they are solutions, J. Math. Phys. **13**, 1745 (1972).

[25] S. Zhou, S. Michalakis, and T. Gefen, Optimal protocols for quantum metrology with noisy measurements, PRX Quantum **4**, 040305 (2023).

[26] H. Cramér, *Mathematical Methods of Statistics* (Princeton University, Princeton, NJ, 1945).

[27] C. R. Rao, Information and the accuracy attainable in the estimation of statistical parameters, Bull. Cal. Math. Soc. **37**, 81 (1945).

[28] V. Giovannetti, S. Lloyd, and L. Maccone, Advances in quantum metrology, Nat. Photon. **5**, 222 (2011).

[29] S. L. Braunstein and C. M. Caves, Statistical distance and the geometry of quantum states, Phys. Rev. Lett. **72**, 3439 (1994).

[30] M. Szczykulska, T. Baumgratz, and A. Datta, Multi-parameter quantum metrology, Adv. Phys.: X **1**, 621 (2016).

[31] R. A. Fisher and E. J. Russell, On the mathematical foundations of theoretical statistics, Philos. Trans. R. Soc. A **222**, 309 (1922).

[32] J. Liu, H. Yuan, X.-M. Lu, and X. Wang, Quantum Fisher information matrix and multiparameter estimation, J. Phys. A: Math. Theor. **53**, 023001 (2019).

[33] P. Horodecki, Ł. Rudnicki, and K. Życzkowski, Five open problems in quantum information theory, PRX Quantum **3**, 010101 (2022).

[34] L. Schwartz, Transformation de Laplace des distributions, Commun. Sém. Math. Univ. Lund **1952**, 196 (1952).